DEVELOPMENT OF SHEAR-WAVE VELOCITY PROFILES AND KAPPA COMPATIBLE WITH GROUND MOTION MODEL FOR TAIWAN

Van-Bang Phung[1], Bor-Shouh Huang[2], Chin-Hsiung Loh[3], Dinh-Hai Pham [4]

[1,2]*Institute of Earth Science, Academia Sinica, Taiwan*

[3]*National Taiwan University, Taiwan*

[4] *HaNoi University of Civil Engineering*

Email: [1] phungvb@earth.sinica.edu.tw, [2] hwbs@earth.sinica.edu.tw

DOI: https://doi.org/10.59382/pro.intl.con-ibst.2023.ses1-5

ABSTRACT: A new velocity model (GMM) compatible with a ground motion prediction model (GMM) for Taiwan is presented in this study. The model is developed using the data set extracted from the flatfile compiled for Taiwan Senior Seismic Hazard Analysis Committee (SSHAC) level 3 project (NCREE, 2015). The Phung et al. (2020) ergodic Sa GMM was used as a backbone model for estimating the site amplification in the frequency domain using inverse Random vibration theory (IRVT). The main motivation for developing a velocity model is that the estimation of the site scaling in terms of the time-averaged shear-wave velocity over the top 30 m (V_{S30}), the method also provides the corresponding depth-dependent $V_S(z)$ profiles and the value for the selected V_{S30} value as a result of the inverse quarter-wave-length method (IQWL). Not all of the empirical amplification can be explained by the 1-D V_S profiles andvalues. For soft sites (V_{S30} < 500 m/s), and intermediate periods (0.5-2.0 sec), there is additional amplification in the empirical data which is attributed to 3-D path and site effects. Using the proposed method, the resulting GMM provides a V_S profile, k, and 3-D effect for each V_{S30} value, which provides a more informative handoff of ground-motion information for use in site-specific site response studies.

KEYWORDS: Ground Motion Models, Inverse Random Vibration Theory, Inverse Quarter Wave Length, Shear-Wave Profiles, Site Amplification, and kappa.

1. INTRODUCTION

The ground motion prediction model (GMM) calculates the median ground motion as a function of the earthquake's magnitude, source-to-site distance, faulting style, and local site conditions. In areas with a large number of ground motion recordings, like Taiwan, GMMs are typically constructed using empirical data. The time-averaged shear wave velocity over the top 30 m of the site profile (V_{S30}) is commonly used in modern GMMs to describe site conditions. To represent the basin effects, additional parameters such depth to shear wave velocities of 1.0 or 2.5 km/s are used. Although useful, the use of V_{S30} as the primary site predictor parameter to site response in GMMs has some significant limitations. Sites with the same V_{S30} value but differing shear wave velocity profiles above the top 30 m of the profile cannot be distinguished by the site response model in GMMs. Another limitation of using V_{S30} in GMMs is that it does not adequately account for variations in the high-frequency spectral content that might occur for locations with the same V_{S30} value and are typically attributed to damping in the shallow crust (kappa).

Although site effects in GMMs are typically characterized by the V_{S30}; however, the V_{S30} is not a fundamental parameter for site amplification. The V_{S30} scaling in the GMM is only applicable to sites for which the site-specific $V_S(z)$ profile is consistent with the average $V_S(z)$ profile represented by GMM for the given V_{S30} value. Therefore, the full $V_S(z)$ profile and kappa are required to estimate the site factors implied by the V_{S30} scaling in GMMs. This concept is used as part of the V_S – correction approach to adjusting GMMs from one region to another (Williams & Abrahamson, 2021). Given the two V_S profiles (one for GMM and one for a site), the ratio of the site amplification is used to adjust ground motion from the GMM to the site-specific ground motion according to the following equation:

$$SA_{site}(T) = \left(\frac{AMP_{site-Vs}(T)}{AMP_{GMM-Vs}(T)}\right) SA_{GMM}(T) \quad (1)$$

Most empirical GMMs do not provide the $V_S(z)$ profile and the k, so they are estimated by the user of the GMM which can have large uncertainties and may be inconsistent with the scaling in the GMM.

Rather than have the users of GMMs estimate these parameters, a better approach is for GMMs to include the $V_S(z)$ profile and the kappa that is consistent with the V_{S30} scaling in the GMM. In this paper, we propose a procedure for developing the V_{S30} – dependent 1-D velocity profiles and kappa values as part of the GMM development, rather than estimating the V_S profile and kappa independent of the development of the GMM. A subset of the ground motion data from earthquakes in Taiwan is used for this application. The selected dataset includes 14535 ground motions from 188 earthquakes in the magnitude range of M3.5 - M7.6 (Figure 1a) recorded at 800 sites (Figure 1b) in the distances range of 0 - 300 km. The ground-motion measure selected for the analysis is the 5% damped spectral acceleration (SA), which is computed as the RotD50 i.e., the median single component horizontal ground motion across all nonredundant azimuths.

2. APPROACH FOR DEVELOPING GMMS WITH COMPATIBLE VS-PROFILES

The traditional approach for developing GMMs is to conduct the regression one frequency at a time for all V_{S30} values, but the 1-D velocity profile for a given V_{S30} value affects the site amplification at all periods. We use an iterative method that alternate between period-by-period GMM development for all V_{S30} values and V_{S30}-by-V_{S30} 1-D V_S profile development for all period. The steps in this approach are listed below:

Step 1: Development of GMMs

Develop an initial GMM for the 5% damped spectral acceleration (SA) with the site factor relative to a rock site condition (V_{S30}=1130 m/s) including random effects for the site and event terms. To demonstrate the methodology, a simple functional form is used:

$$\begin{aligned} ln\big(SA(T)\big) = \\ a_1 + a_2(M-6) + a_3(M-8.5)^2 \\ +\big(a_4 + a_5(M-6)\big) \\ \cdot ln\big(R_{rup} + 5 \cdot e^{0.4\cdot(M-6)}\big) + a_6 R_{rup} \\ +f_{site}(V_{S30}) + f_{basin}(z_{1.0}) \\ +f_{NL-site}(V_{S30}, SA_{1130}) \\ + \delta B + \delta S2S + \delta W \end{aligned} \quad (2)$$

where M is moment magnitude; R_{rup} is the rupture distance; V_{S30} is the average shear-wave velocity over the top 30 m; $z_{1.0}$ is the basin depth parameter; $\hat{z}_{1.0}$ is average basin depth inferred from Ph20 given V_{S30}; δB, δS2S and δW are the between event residual, between site residual, and single site residual, respectively. The $f_{NL-site}$ term models the non-linear site effects and is fixed to the non-linear site term given by Phung et al. (2020). The term $f_{site}(V_{S30})$ and $f_{basin}(Z_{1.0})$ in Eq. 2 represent the site amplification in soil deposits, which were chosen based on plots of site amplifications (relative to rock site condition, V_{S30} = 1130m/s). The equations for the site terms are expressed bellow:

$$f_{site}(V_{S30}) = \phi_1 \cdot min\left(ln\left(\frac{V_{S30}}{1130}\right), 0\right) \quad (3)$$

$$\begin{aligned} f_{basin}(z_{1.0}) = \phi_{5a} \cdot ln\big(min(Z_{1.0}, 100)\big) \\ +\phi_{5b} \cdot ln\big(max(Z_{1.0}, 100)\big) \end{aligned} \quad (4)$$

We adopt a nonlinear mixed effect regression (Bate et al. 2014) with two random effects (given to the event and site terms) to avoid biases in site terms due to unbalanced data (i.e., the number of soft soil sites is much larger than the number of hard sites). Once the random effects regression was carried out, the regression parameters and the residuals can be obtained, which then constitutes the GMM.

Step 2: Development of Total Site Response in FAS Domain

The inverse random vibration theory (IRVT) approach described in Al Atik (2013) is used to derive FAS compatible with the Taiwan Ph20 GMM response spectra for strike slip scenarios with magnitude 5, 6, and 7, and rupture distance (Rup) of 5, 10, 20 km. Depth to top of rupture is calculated using the CY14 relationship as a function of magnitude and style of faulting. Default depth to horizontal Vs of 1.0 km/s is used. Short distances scenarios were selected to minimize the effects of anelastic attenuation Q on the ground motion. Median response spectra are estimated from the GMM for the nine scenarios listed above for a set of V_{S30} = 360, 490, 620 and 760 m/s. For each scenario, FAS are computed using the IRVT approach, as implemented in Python Albert Kottke. (2020) for each site condition. Input parameters to IRVT including duration is calculated using estimate of source and path durations based on Boore and Thomson (2015). Peak factor of Vanmarcke (1975) is used in the IRVT method. For V_{S30} = 760 m/s, Figure 2 shows an illustrative example for converting 5% damped response spectral acceleration (SA) into Fourier amplitude spectra (FAS) computed from the selected nine scenarios. The conversion was done using IRVT method in which the linear site response of the GMM in FAS domain relative to V_{S30} of 1000 m/s. For each scenario, the ratio of the FAS at a specific V_{S30} relative to the reference FAS (V_{S30} = 1000 m/s) of the corresponding scenario is computed. Figure 3a shows the ratio of FAS for the nine scenarios to those at 1000 m/s. This ratio

represents the linear site response of the GMM in the FAS domain relative to a reference V_{S30} of 1000 m/s.

The relative site response is computed by averaging those of the nine scenarios, which is then smoothed as a function of period. These relative site response functions include the combined effects of linear site amplification relative to V_{S30} of 1000 m/s and relative kappa effects.

The relative site response shown in Figure 3a is then converted into the total site response relevant to the source depth (V_S = 3500 m/s). This is done by multiplying the relative site response with the linear site amplification with kappa effect of the reference profile of V_{S30} = 1000 m/s as shown in Figure 3b. This reference profile was adopted from Boore (2016) for WUS. The resulting total site response relative to V_S = 3500 m/s shown in Figure 3c for a set of V_{S30} = 360, 490, 620, 760 and 1100 m/s. These total site response functions contain the effects of both linear site amplification and kappa which are then referred to as FAS -domain site response of the GMM at the different V_{S30} values.

Step 3: Derivation of GMM – Compatible VS profiles

The site amplification from step 2 has the combined effect of the amplification due to the V_S profile and the attenuation due to κ_0. For a set of V_{S30} values, the effect of κ_0 is removed. The kappa-corrected amplification is used to invert for the 1-D Vs profile for each V_{S30} using the inverse quarter-wavelength (QWL) method described by Al Atik & Abrahamson (2021). An example of this process is shown in Figure 4 for V_{S30} =7 60 m/s. Starting

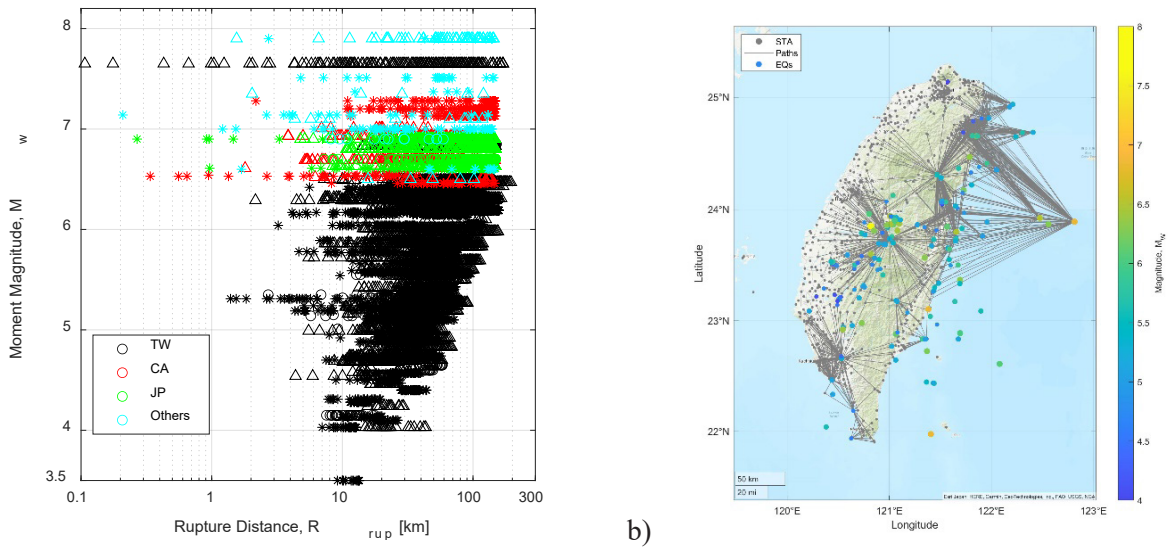

a) b)

Figure 1. a) Magnitude and distance distribution of the ergodic Ph20 GMM dataset, b) Events and stations distribution used in the developement of the ergodic Ph20 GMM

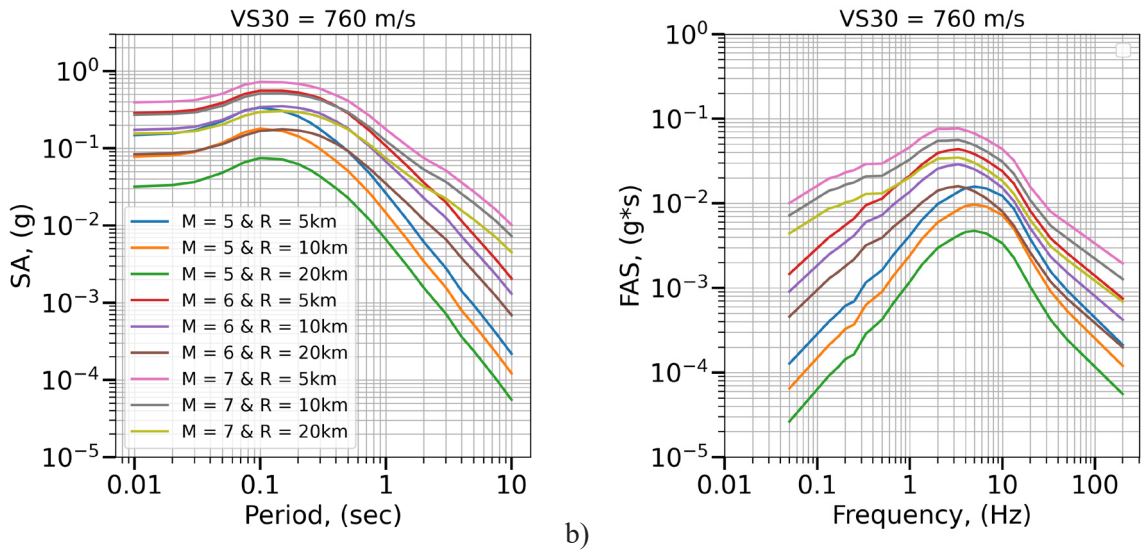

a) b)

Figure 2. An illustrative example for converting 5% damped response spectral acceleration (SA) into Fourier amplitude spectra (FAS) computed from nine scenarios for V_{S30} = 760 m/s

with the site amplification shown in Figure 3c (V_{S30} = 760 m/s curves), an estimate of kappa is estimated from the slope of the high-frequency range between 5.0 and 20 Hz (pink curve) by fitting Eq. 5 to the site amplification. The kappa-corrected amplification is then computed, as shown by the blue curve in Figure 4a (blue curve). Note that Eq. 5 represents an assumption of a power law function in the top 30 m of the profile.

$$A(f) = \left[\frac{\rho_R \cdot V_{S_R} \cdot 0.03^b / V_{S30}}{\left(\rho_1 - \frac{V_{S30} \cdot \rho_2 \cdot (4 \cdot 0.03^b \cdot f / V_{S30})^{b/b-1}}{0.03^b \cdot (b^2 - 1)}\right) * \left(\frac{4 \cdot 0.03^b \cdot f}{V_{S30}}\right)^{b/b-1}}\right]^{1/2} e^{(-\pi\kappa f)} \quad (5)$$

In which, V_{S_R} and ρ_R are the velocity and density at source depth (3500 m/s). Two unknown parameters are b and κ which is estimated by fitting Eq. 5 to the site amplification for each VS30 value. The inverted Vs profile is shown in Figure 4b. These same steps are applied to each V_{S30}. As can be seen from Figure 4b, the V_{S30} of inverted V_S profiles for soil sites is much less than the specified value. This inconsistency is addressed in Step 4.

Step 4: Constrain the Vs profile at the top 30 m

Apply constraints to the V_S profile in the top 30 m so that V_{S30} value from the inverted V_S profile is consistent with the specified V_{S30} and to the profile at depth so that it matches the median $z_{1.0}$ values from Taiwan. The resulting V_S profiles for a set of V_{S30} are shown in Figure 5. Figure 6 presents a comparison of the derived 1D V_S profiles from the Taiwan GMMs with those from the NGA-West 2 GMM for V_{s30} = 620 and 760 m/s. Figure 4 highlights the differences among the derived 1D reference V_S profiles for the Taiwan as well as the difference between the NGA-West2 profiles. These differences are observed at all depth of the profiles. The site amplification is computed using the QWL amplification with a scale factor to account for the differences between the amplification computed

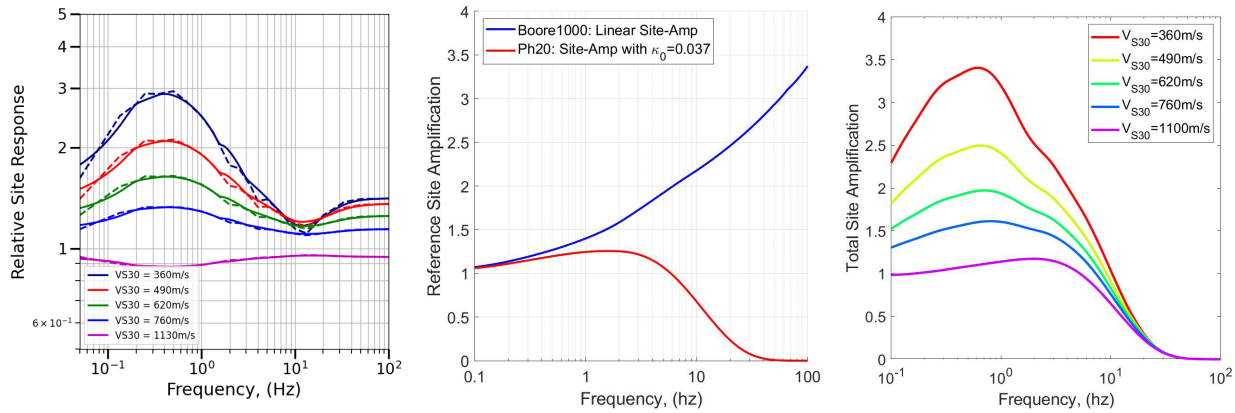

a) b) c)

Figure 3. Derivation of the total site amplification relative to a hard-rock site condition with V_S=3500 m/s. (a) Relative site amplification to reference site condition (V_{S30} = 1000 m/s), (b) reference linear site amplification (V_{S30}=1000m/s), and (c) the total site amplification for V_{S30} = 360, 490, 620, and 760 m/s

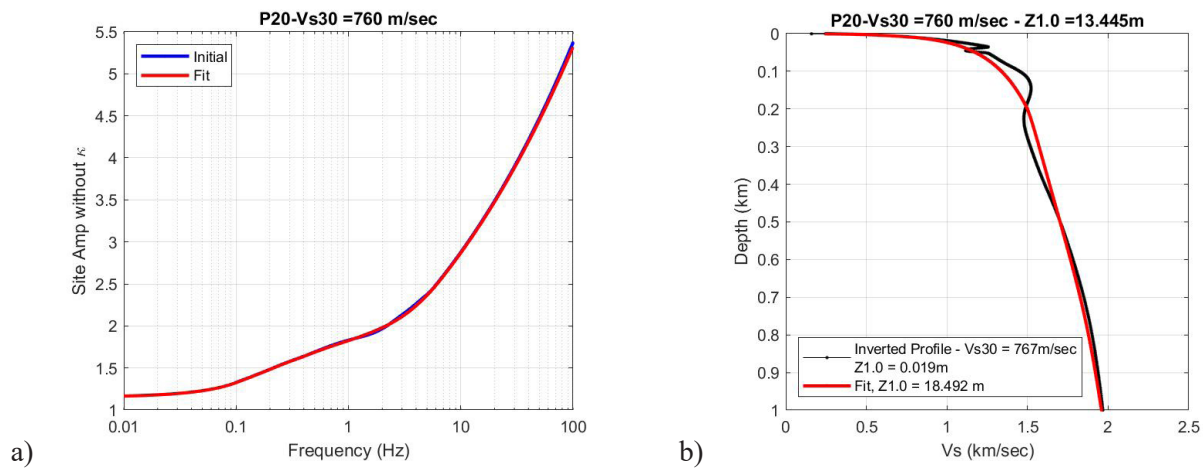

a) b)

Figure 4. Steps for the derivation of the kappa and kappa-corrected site amplification as input for the IQWL method: a) total site amplification with and without kappa, b) the inverted Vs-profile and its corrected version

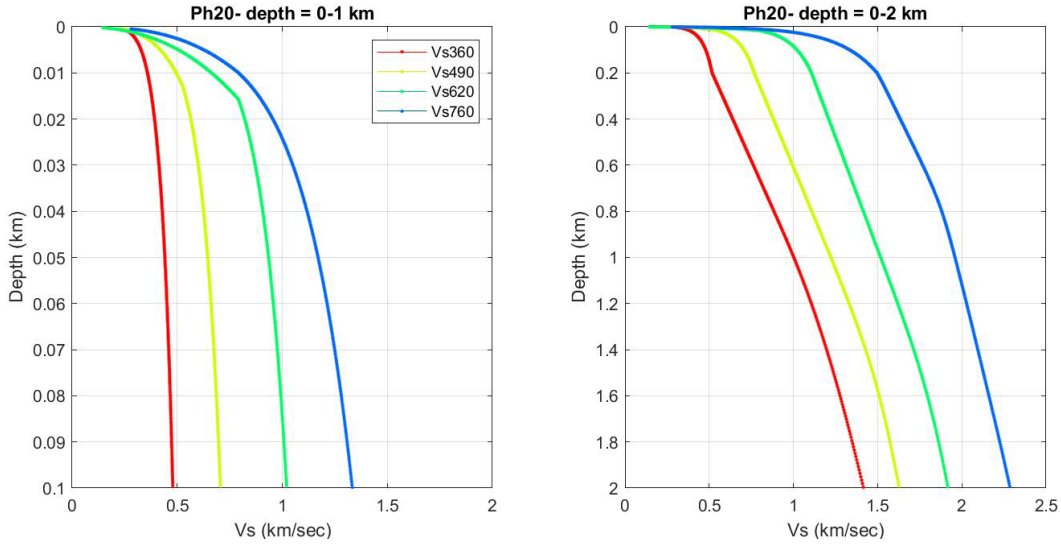

Figure 5. The V_{S30}-consistent V_S-profiles for a suite of V_{S30} values of 360, 490, 620 and 760 m/s

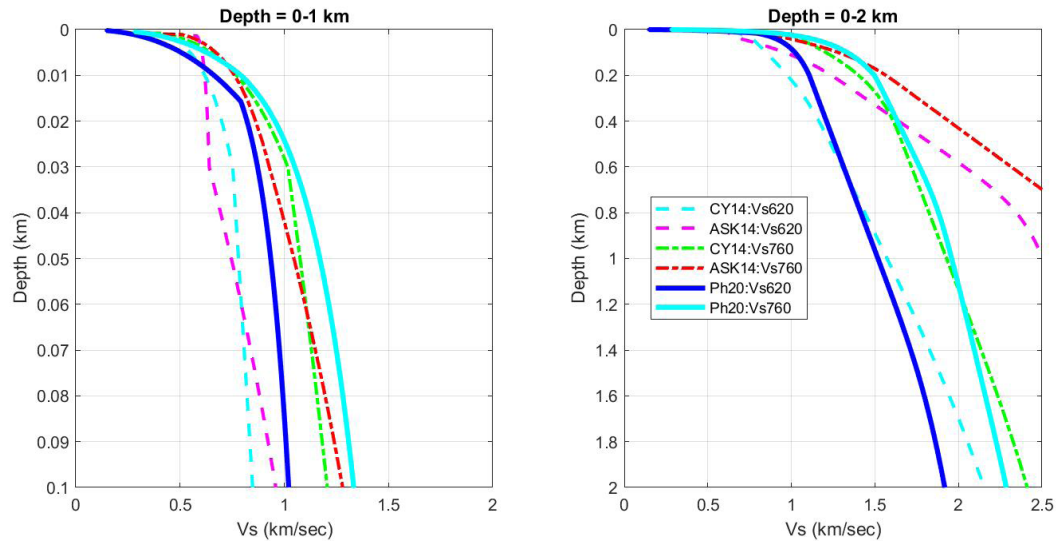

Figure 6. Comparison of derived 1D host V_S profiles for Taiwan GMMs with the NGA-West2 GMMs for V_{S30} = 620 and 760 m/s.

using the QWL method and the amplification computed using a traditional site response from a 1-D profile. GMMs typically model the V_{S30} scaling as a simple linear function of the ln (V_{S30}) at a given frequency. The inverted profiles are approximately linear with for the central V_{S30} range, but there is curvature that we include in the model as a non-parametric model in the GMM.

Step 5: Estimate the 1D Site response

Comparison of the site response for the derived host V_S profiles and kappa values to the initial GMM's site response are shown in Figure 7. Figure 7 indicates that the derived host Vs profiles and kappa value for Ph20 match well with the GMM's site response for the stiff site conditions with V_{S30} > 620 m/s. For the softer sites, Ph20's site response cannot be fully represented with a 1D

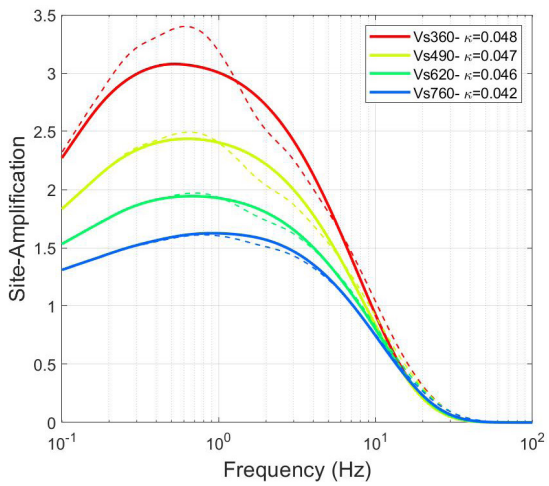

Figure 7. Comparison of Ph20's site amplification with that obtained using the derived 1-D Vs profiles and kappa values for V_{S30} = 360, 490, 620, and 760 m/s

V_S profile that constrains the assigned V_{S30} values. We have made a conclusion that for the softer site conditions than it is for the stiffer ones, the 2D or 3D site reaction that is recorded in empirical ground motion data is stronger. The GMM's site response and that produced with the derived 1D V_S profiles for the softer site conditions are likely incompatible due to these 2D or 3D effects, which also make it challenging to appropriately use empirical site response with 1D Vs profiles.

3. CONCLUSIONS

The methodology given in this paper provides a method for GMM developers to include the estimation of the $V_S(z)$ profile and κ as a part of the GMM development. In addition to providing the information needed for the $V_S - \kappa$ correction approach, providing $V_S(z)$ profiles as part of the GMM will help to clarify that the V_{S30} value is just an index for a $V_S(z)$ profile and not a fundamental parameter of site amplification. A key result of the example application of the approach is that the empirical site amplification at long periods for soft sites cannot be fully explained by 1-D site response. The 1-D V_S profiles can explain by about 80% of the total site amplification relative to hard-rock. We attributed this underestimation of the long-period amplification to 3-D effects. The total amplification (1-D plus 3-D effects) can be up to a factor of 1.5 larger than the amplification due only to 1-D effects.

There are potential implications of the underprediction of the site amplification using the inverted 1-D profiles that need further study. A common approach in seismic hazard is to use rock motion as the input to 1-D soil profile. There are only small 3-D effects for soft-rock sites, so the input motion will not have 3-D effects. Using a site-specific 1-D profile to compute the site amplification relative to the input rock motion will not capture the 3-D effects. This leads to the question: are there missing 3-D effects in the input motion at depth for soil sites? The alternative, is that there is a bias in our approach. Further work is needed to resolve the physical cause of the unexplained amplification for soil sites.

ACKNOWKEDGMENTS

This research is supported by Ministry of Science & Technology (MOST) of Taiwan under contract of MOST 108-2116-M-001-011, MOST 108-2116-M-001-MY3, and MOST 109-2119-M-001-011. We would like to thank National Center for Research on Earthquake Engineering (NCREE) for proving the ground motion data of this study.

REFERENCES

[1] Al Atik, L., & Abrahamson, N. (2021). A Methodology for the Development of 1D Reference V_S Profiles Compatible with Ground-Motion Prediction Equations: Application to NGA-West2 GMPEs. *Bulletin of the Seismological Society of America,* 111(4), 1765–1783. https://doi.org/10.1785/0120200312.

[2] Albert Kottke. (2020). Srkottke/pyrvt v0.7.2 (v0.7.2). Zenodo. https://doi.org/10.5281/zenodo.3630729.

[3] Boore, D. (2016). Determining generic velocity and density models for crustal amplification calculations, with an update of the Boore and Joyner (1997) Generic Site Amplification for Graphic Site Amplification. In *Bulletin of the Seismological Society of America* (Vol. 106, Issue 1, p. 316320). https://doi.org/10.1785/0120150229.

[4] Bates, D., Mächler, M., Bolker, B., & Walker, S. (2014). *Fitting Linear Mixed-Effects Models using lme4* (arXiv:1406.5823). arXiv. https://doi.org/10.48550/arXiv.1406.5823.

[5] Boore DM, Thompson EM (2015). Revisions to some parameters used in stochastic-method simulations of ground motion. *Bull Seismol Soc Am* 105(2A):1029–1041.

[6] NCREE. (2015). *Reevaluation of Probabilistic Seismic Hazard of Nuclear Facilities in Taiwan Using SSHAC Level 3 Methodology Project.* Available at: Http://sshac.ncree.org.tw (accessed 31 December 2019). National Center for Research on Earthquake Engineering (NCREE).

[7] Kamai, R., Abrahamson, N. A., & Silva, W. J. (2016). VS30 in the NGA GMPEs: Regional Differences and Suggested Practice. *Earthquake Spectra*, 32(4), 2083–2108. https://doi.org/10.1193/072615EQS121M.

[8] Phung, V.-B., Loh, C. H., Chao, S. H., & Abrahamson, N. A. (2020). Ground motion prediction equation for Taiwan subduction zone earthquakes. *Earthquake Spectra*, 36(3), 1331–1358. https://doi.org/10.1177/8755293020906829.

[9] Vanmarcke EH (1976). Structural response to earthquakes. In: *Developments in geotechnical engineering,* vol 15. Elsevier, pp 287–337.

[10] Williams, T., & Abrahamson, N. (2021). Site-Response Analysis Using the Shear-Wave Velocity Profile Correction Approach. *Bulletin of the Seismological Society of America,* 111(4), 1989–2004. https://doi.org/10.1785/0120200345.